Robust Pupil Boundary Detection by Optimized Color Mapping for Iris Recognition

Rasoul Kheirolahy, Hossein Ebrahimnezhad and MohammadHossein Sedaaghi
Department of Electrical Engineering, Sahand University of Technology, Tabriz, Iran.
r_kheirolahy@sut.ac.ir, ebrahimnezhad@sut.ac.ir, sedaaghi@sut.ac.ir

Abstract

Accurate pupil segmentation is the first and most important step for an iris recognition system. Current methods are based on fitting a model such as circle or ellipse to find and detect pupil, while these methods don't have sufficient accuracy and are sensitive to the specular spot reflection. In this paper, we utilize an optimized color mapping to increase the accuracy of pupil segmentation, regardless of pupil model and its shape (circular or elliptic), while removing the effects of specular spot reflection. The optimum color mapping can be established by an iterative minimization algorithm similar to Levenberg-Marquardt (LM) method. By applying this method, a new image is provided with a clear pupil region that can be easily segmented. Also a robust preprocessing step is presented in this paper that sharpens and clears pupil region. We obtain 98% accuracy in pupil boundary detection by applying this method on UBIRIS dataset. Also, the proposed method works well on any model of eye image even where the eye is not perpendicular to the camera.

1. Introduction

In people recognition based on biometric features, Iris recognition has become more important in recent years and the accurate pupil detection, as the inner iris boundary, is the most important and the first step in iris recognition system. Pupil's shape is rather similar to a dark disc and therefore, a simple pupil detection method tries to search for a circular black disc in the image. In general, current methods for iris boundary detection are based on texture and shape; the two reference methods are Daugman and Wildes's methods. In former method an integro differential operator is used to detect the iris boundary [1]. However, it is sensitive to the specular spot reflection. The latter applies Hough transform in a binary edge point to estimate particular contour parameter values such as circle or ellipse [2-4]. Most of other researches originate from these two methods and use edge detection and image thresholding as preprocessing steps for iris boundaries detection. For example, Cui [5] has used wavelet and then Hough transform. Kim [6] has employed Gaussian mixture model for defining three regions: dark, middle and bright. Then, he uses Hough transform for pupil boundary detection. In [7], Lima et.al. compute the summation of intensities along each row and column and choose the row and column with minimum value as the center of the pupil. Then they use edge detection and Hough transform to detect pupil boundary. In [8], Jafar et. al. employ median filter to remove garbage point and apply edge detection using LOG (Laplacian of Gaussian) operator, then by counting the number of black pixels in each row and column and using the first and end position of black pixel, the center and radius of the pupil is estimated. In [6], the area and circularity of the black region are found as two features. Then, morphological operation is used to segment the pupil. In [7], pupil boundary detection is done using morphological operators where adaptive histogram equalization is used to sharpen the intensity between iris and pupil. In [9], an active contour is used for pupil boundary detection where the external force of its energy minimization is based on Daugman's integro differential operator. The proposed method for pupil segmentation in [12] is based on dividing image into some rectangle regions and computing the mean intensity in each region, then a region with minimum value is selected as the reference for pupil and the pupil boundary is defined by expanding this region. Also an efficient approach for pupil detection, applied in CASIA iris image database [13], is presented in [14] by Dey,s and samanta,D, that use edge detection after down scaling and power transform for finding the best radius and center of circle matched to the connected edge point as the radius and center of pupil.

Almost all of these methods are applied for a limited set of datasets that are in gray level mode and not in color images. Also these methods are not efficient against specular spot reflection and search a circular or an elliptic model for pupil boundary, hence cannot find

correct boundary pupil with arbitrary (non circle or ellipse) shape.

In this paper, we propose a combinatory method to segment pupil boundary. At first, we apply adaptive histogram thresholding and morphological filtering as a robust preprocessing step to find an estimated region of pupil and then isolate this region using Hough transform [3], [4] and fit a circle. In the next step, we find an optimized color mapping that maximizes the color difference between inside and outside the initially segmented region as pupil. We find the optimized color mapping using iterative Levenberg-Marquardt method [15]. The resulted image in new color map has a clear pupil region without specular spot reflection. To clarify the efficiency of our method we also compare this method by the two main methods, Daugman's integro differential method and circular hough transform algorithm, in some feature terms.

2. Preprocessing

We use Wildes's method [3] in order to obtain an initial estimation of the pupil region. Since pupil is similar to a dark disc and majority of pixels in this region have low intensity, the first valley in the histogram is considered as a proper threshold to remove non pupil region. So, the higher intensity pixels (than the above threshold) are changed to 255 in three color plane (as it is assumed to have a color eye image). In the next step, the histogram of each color plate is mapped into the range between 0 to 255. The resulting image is shown in Figures 1-b and 2-b. Finally, by using morphological reconstruction and smoothing, as illustrated in Figures 1-c and 2-c, and Hough transform [3,4], pupil position can be approximately determined.

3. Initial segmentation

The resulting image from preprocessing step is used as input for Wildes's algorithm [2] to determine initial pupil segmentation. In this method contour fitting is done in two steps: first converting the image intensity information into a binary edge-map and then voting the edge points to instantiate particular contour parameter values. The edge map is recovered via gradient-based edge detection [16], [17]. This operation consists of thresholding the magnitude of the image intensity gradient:

$$\left|\nabla G\left(x,y\right)*I\left(x,y\right)\right| \qquad with:$$
$$G\left(x,y\right)=\frac{1}{2\pi\sigma^2}\exp\left(-\frac{\left(x-x_0\right)^2+\left(y-y_0\right)^2}{2\sigma^2}\right) \tag{1}$$

G(x,y) is a two-dimensional Gaussian with center $\left(x_0,y_0\right)$ and standard deviation σ that smoothes the image to select the spatial scale of edges under consideration. The voting procedure is done via Hough transform [3], [4]. For the circular boundary, a set of the recovered edge points $\left(x_j,y_j\right), j=1:n$ exists. The Hough transform is defined as follows [2]:

$$H\left(x_c,y_c,r\right)=\sum_{j=1}^{n}h\left(x_j,y_j,x_c,y_c,r\right) \tag{1}$$

where:

$$h\left(x_j,y_j,x_c,y_c,r\right)=\begin{cases}1, & \text{if } g\left(x_j,y_j,x_c,y_c,r\right)=0\\ 0, & \text{otherwise}\end{cases}$$

with: (3)

$$g\left(x_j,y_j,x_c,y_c,r\right)=\left(x_j-x_c\right)^2+\left(y_j-y_c\right)^2-r^2$$

For each edge point $g\left(x_j,y_j,x_c,y_c,r\right)=0$ for every $\left(x_c,y_c,r\right)$ where they represent a circle through that point. Correspondingly, the parameter triple that maximizes H is common to the largest number of edge points and is a reasonable choice to represent the contour of interest.

This method provides an estimation of the pupil region in the image and initial contour for next step to find an optimum color mapping. To increase the precision of pupil boundary detection, we use an optimum color transform that maximizes the mean color differences between inside and outside of the primary contour so that the mapped image clearly determines the pupil boundary in any shape.

4. Optimized color mapping algorithm for accurate pupil segmentation

Wildes's method [2] and circular Hough transform [3,4] are not precise enough in pupil boundary detection and have poor performance against specular spot reflection of non diffused artificial light. Therefore, we use them as an elementary method to estimate pupil region. Optimized color mapping matrix which is shown in Eq.4 is computed based on an iterative method similar to Levenberg-Marquardt (LM) algorithm.

$$\begin{bmatrix}r'\\g'\\b'\end{bmatrix}=\begin{bmatrix}a_{11}&a_{12}&a_{13}\\a_{21}&a_{22}&a_{23}\\a_{31}&a_{32}&a_{33}\end{bmatrix}=\begin{bmatrix}r\\g\\b\end{bmatrix}\equiv M_{3*3}\times\begin{bmatrix}r\\g\\b\end{bmatrix} \tag{4}$$

Where, M is color mapping matrix with parameter $\theta=\left[a_{11},a_{21},a_{31},a_{12},a_{22},a_{32},a_{13},a_{23},a_{33}\right]$ which is calculated by optimization LM algorithm; and (r',g',b') and (r,g,b) are color plates of the mapped and original images, respectively. In fact, using LM

algorithm we maximize the color difference angle or minimize the following error function:

$$e = \left(\frac{\vec{A}.\vec{B}}{\left|\vec{A}\right|\left|\vec{B}\right|} \right) = \cos(\alpha) \tag{5}$$

where:

$$\begin{aligned} \vec{A} = & \left[\frac{1}{nr'_{inside}} \sum_{m=1}^{row} \sum_{l=1}^{col} r'(m,l)_{inside} \right] \vec{i} \\ & + \left[\frac{1}{ng'_{inside}} \sum_{m=1}^{row} \sum_{l=1}^{col} g'(m,l)_{inside} \right] \vec{j} \\ & + \left[\frac{1}{nb'_{inside}} \sum_{m=1}^{row} \sum_{l=1}^{col} b'(m,l)_{inside} \right] \vec{k} \end{aligned} \tag{6}$$

$$\begin{aligned} \vec{B} = & \left[\frac{1}{nr'_{outside}} \sum_{m=1}^{row} \sum_{l=1}^{col} r'(m,l)_{outside} \right] \vec{i} \\ & + \left[\frac{1}{ng'_{outside}} \sum_{m=1}^{row} \sum_{l=1}^{col} g'(m,l)_{outside} \right] \vec{j} \\ & + \left[\frac{1}{nb'_{outside}} \sum_{m=1}^{row} \sum_{l=1}^{col} b'(m,l)_{outside} \right] \vec{k} \end{aligned} \tag{7}$$

In the above equations, nr', ng', nb' denote the total number of pixels, inside and outside of the initial contour for each color plate, and $\vec{A}, \vec{B}$ are color vectors for inside and outside of the initial contour. The mapped image (r', g', b'), clearly defines the pupil region and its boundary with reduced effect of specular spot reflection as illustrated in Figures 1-e and 2-e. Note that the defined pupil region can be ellipse or circle or any possible shape. The accurate pupil boundary can simply be determined from mapped image by smoothing this image as pointed out in Figures 1-f and 2-f and applying the Canny edge detector on the smoothed mapped image as demonstrated in Figures 1-g and 2-g. Finally by removing the small and short edges, we get accurate pupil boundary.

4.1. Optimized color mapping using LM

The error function in Eq. 5 can be minimized using an iterative method similar to the Levenberg-Marquardt algorithm [15], explained in three basic steps:

1. With an initial estimate, calculate the Hessian matrix $\mathbf{H}$ and the difference vector $\mathbf{d}$:

$$\mathbf{H} = \begin{bmatrix} \mathbf{h_{11}} & \mathbf{h_{12}} & \mathbf{h_{13}} \\ \mathbf{h_{21}} & \mathbf{h_{22}} & \mathbf{h_{23}} \\ \mathbf{h_{31}} & \mathbf{h_{32}} & \mathbf{h_{33}} \end{bmatrix} \tag{8}$$

with:

$$\mathbf{h_{11}} = \begin{bmatrix} \frac{\partial e}{\partial a_{11}}.\frac{\partial e}{\partial a_{11}} & \frac{\partial e}{\partial a_{11}}.\frac{\partial e}{\partial a_{21}} & \frac{\partial e}{\partial a_{11}}.\frac{\partial e}{\partial a_{31}} \\ \frac{\partial e}{\partial a_{21}}.\frac{\partial e}{\partial a_{11}} & \frac{\partial e}{\partial a_{21}}.\frac{\partial e}{\partial a_{21}} & \frac{\partial e}{\partial a_{21}}.\frac{\partial e}{\partial a_{31}} \\ \frac{\partial e}{\partial a_{31}}.\frac{\partial e}{\partial a_{11}} & \frac{\partial e}{\partial a_{31}}.\frac{\partial e}{\partial a_{21}} & \frac{\partial e}{\partial a_{31}}.\frac{\partial e}{\partial a_{31}} \end{bmatrix}$$

$$\mathbf{h_{12}} = \begin{bmatrix} \frac{\partial e}{\partial a_{11}}.\frac{\partial e}{\partial a_{12}} & \frac{\partial e}{\partial a_{11}}.\frac{\partial e}{\partial a_{22}} & \frac{\partial e}{\partial a_{11}}.\frac{\partial e}{\partial a_{32}} \\ \frac{\partial e}{\partial a_{21}}.\frac{\partial e}{\partial a_{12}} & \frac{\partial e}{\partial a_{21}}.\frac{\partial e}{\partial a_{22}} & \frac{\partial e}{\partial a_{21}}.\frac{\partial e}{\partial a_{32}} \\ \frac{\partial e}{\partial a_{31}}.\frac{\partial e}{\partial a_{12}} & \frac{\partial e}{\partial a_{31}}.\frac{\partial e}{\partial a_{22}} & \frac{\partial e}{\partial a_{31}}.\frac{\partial e}{\partial a_{32}} \end{bmatrix}$$

$$\vdots$$

$$\mathbf{h_{33}} = \begin{bmatrix} \frac{\partial e}{\partial a_{13}}.\frac{\partial e}{\partial a_{13}} & \frac{\partial e}{\partial a_{13}}.\frac{\partial e}{\partial a_{23}} & \frac{\partial e}{\partial a_{13}}.\frac{\partial e}{\partial a_{33}} \\ \frac{\partial e}{\partial a_{23}}.\frac{\partial e}{\partial a_{13}} & \frac{\partial e}{\partial a_{23}}.\frac{\partial e}{\partial a_{23}} & \frac{\partial e}{\partial a_{23}}.\frac{\partial e}{\partial a_{33}} \\ \frac{\partial e}{\partial a_{33}}.\frac{\partial e}{\partial a_{13}} & \frac{\partial e}{\partial a_{33}}.\frac{\partial e}{\partial a_{23}} & \frac{\partial e}{\partial a_{33}}.\frac{\partial e}{\partial a_{33}} \end{bmatrix} \tag{9}$$

and:

$$\mathbf{d} = \begin{bmatrix} \mathbf{d_1} & \mathbf{d_2} & \mathbf{d_3} \end{bmatrix} \tag{10}$$

with:

$$\begin{aligned} \mathbf{d_1} &= \left[e.\frac{\partial e}{\partial a_{11}} \quad e.\frac{\partial e}{\partial a_{21}} \quad e.\frac{\partial e}{\partial a_{31}} \right] \\ \mathbf{d_2} &= \left[e.\frac{\partial e}{\partial a_{12}} \quad e.\frac{\partial e}{\partial a_{22}} \quad e.\frac{\partial e}{\partial a_{32}} \right] \\ \mathbf{d_3} &= \left[e.\frac{\partial e}{\partial a_{13}} \quad e.\frac{\partial e}{\partial a_{23}} \quad e.\frac{\partial e}{\partial a_{33}} \right] \end{aligned} \tag{11}$$

Update the parameter $\hat{\boldsymbol{\theta}}$ by an amount $\boldsymbol{\Delta\theta}$:

$$\hat{\boldsymbol{\theta}}_{(n+1)} = \hat{\boldsymbol{\theta}}_{(n)} + \boldsymbol{\Delta\theta} = \hat{\boldsymbol{\theta}}_{(n)} + \frac{1}{\lambda}\mathbf{H}^{-1}.\mathbf{d} \tag{12}$$

Where λ is a time-varying stabilization parameter.

2. Go back to step 1 until the estimate converges.

5. UBIRIS dataset

UBIRIS [18] database is composed of 1877 images collected from 241 persons during September, 2004 in two distinct sessions. It constitutes the world's largest public and free available iris database at present. A Nikon E5700 camera with software version E5700v1.0, 71mm focal length, 4.2 F-Number, 1/30 sec exposure time, RGB color representation and ISO-200 ISO speed, is used to capture the image. Images dimensions are 2560×1704 pixels with 300 dpi horizontal and vertical resolution and 24 bit depth. They are saved in JPEG format with lossless compression.

6. Experimental results

Implementation of the proposed method on UBIRIS database results in 98% accuracy for pupil boundary detection. Some results of the proposed method applied on UBIRIS database and our database are shown in Figures 1-h and 2-h respectively. Also, the result of our implementation of Wildes's method, are illustrated in Figures 1-d and 2-d. By comparing our method with Wildes's method that uses circular Hough transform for pupil boundary detection and daugman's algorithm, as the two main methods for finding pupil boundary, the results obviously show that those methods cannot detect pupil boundary in accurately, and fails when the shape of the pupil is not circular. Briefly we compare some features in Table1 to clarify accuracy and efficiency of our method to find pupil boundary in any shape**.** Also, as shown in Figures 1-e and 2-e, our method removes the specular spot reflection and the effects of eyelashes that appears as an obstacle in pupil boundary detection.

7. Conclusion

In this paper, we have proposed a robust method for pupil boundary detection, regardless of pupil model and its shape, by computing an optimized color mapping and projecting the color space to a new space. In such mapping, the color angle between the mean of color pixel values inside and outside of the approximate region of the pupil becomes maximum. It leads to a new image with clear pupil boundary. Also, this color mapping removes the effect of specular spot reflection. The optimized color mapping method can be employed along with the iris texture feature to determine the outer iris boundary accurately, as another basic step for iris recognition system.

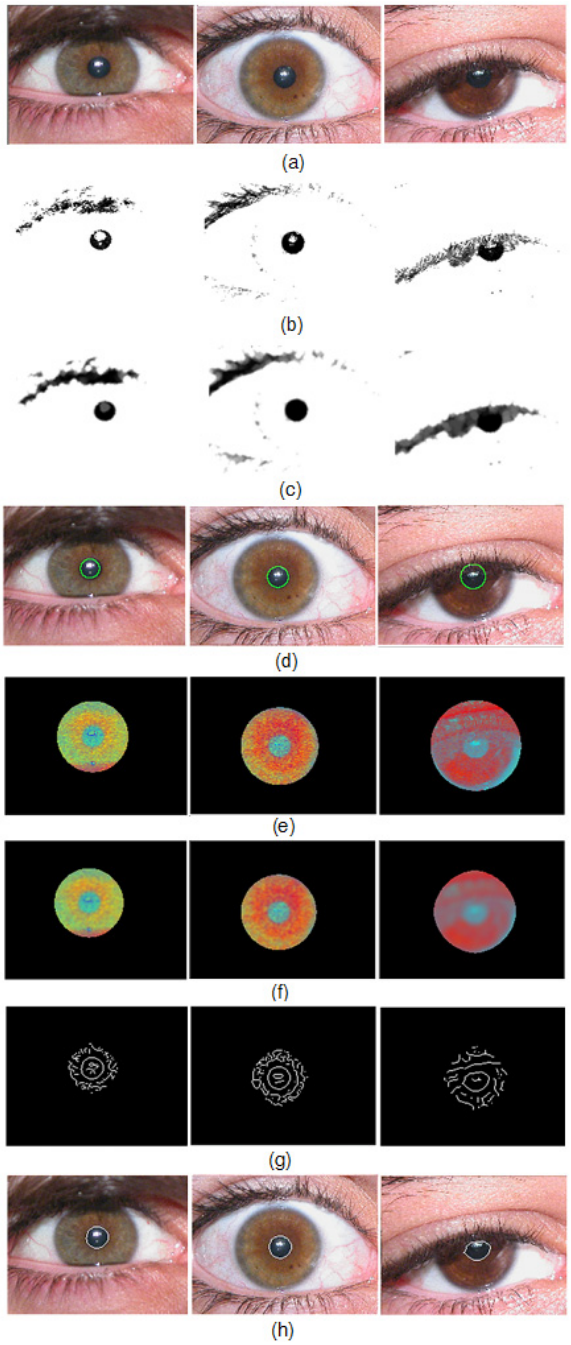

Figure 1. Experimental results on UBIRIS database: (a) the original image, (b) tresholding and then extending the histogram of each of three color plate in the range of 0 to 255, (c) morphological reconstruction and smoothing the image in part b, (d) the result of Wildes's method implementation, (e) the color mapped image, (f) the smoothed color mapped image, (g) edge of the smoothed color mapped image, (h) result of the proposed method.

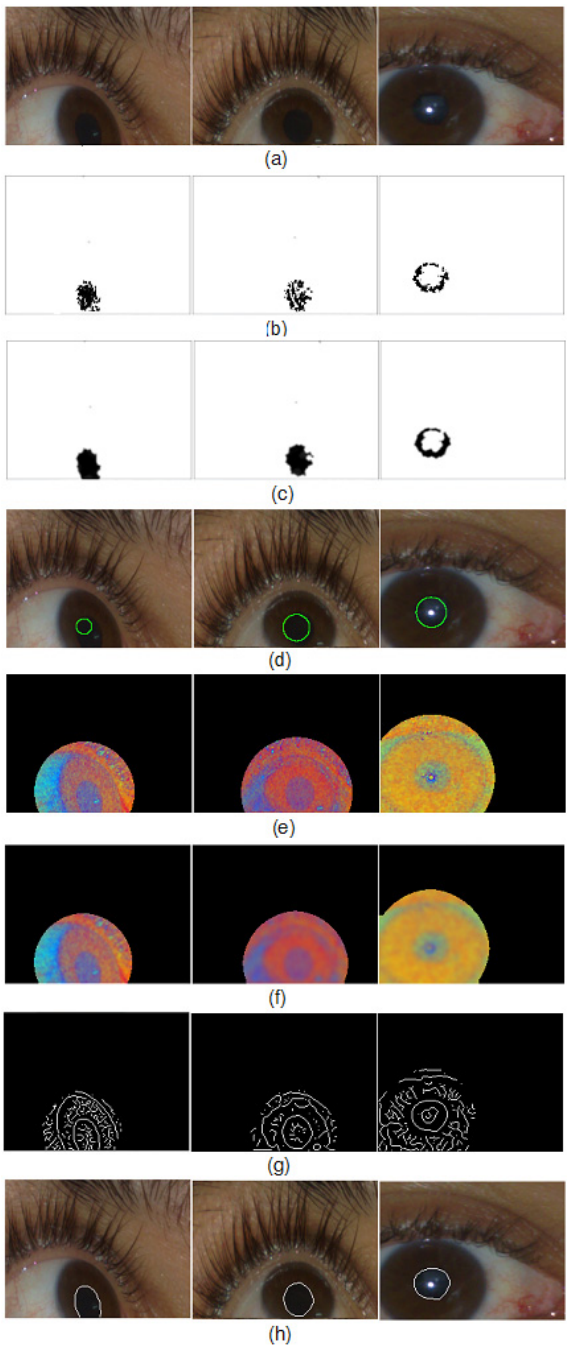

Figure 2. Experimental results on our database: (a) the original image, (b) tresholding and then extending the histogram of each of three color plate in the range of 0 to 255, (c) morphological reconstruction and smoothing the image in part b, (d) the result of Wildes's method implementation, (e) the color mapped image, (f) the smoothed color mapped image, (g) edge of the smoothed color mapped image, (h) result of the proposed method.

TABLE1. Comparing some features of different methods in pupil boundary detection

	Willd's Hough transform	Daugman's Integro differential operator	Proposed method
efficiency in low contrast Iris images	low	low	high
accuracy in pupil boundary detection (circular shape)	average	average	high
accuracy in pupil boundary detection (arbitrary shape)	low	low	high
computational cost	low	low	average
robustness against specular spot reflection	low	low	high

8. References

[1] J. Daugman, "How iris recognition works", *IEEE Trans. on Circuits and Systems for Video Technology*, vol. 14, no. 1, 2004, pp. 21-30.

[2] R. Wildes, "Iris recognition: An emerging biometric technology", *Proceedings of the IEEE,* vol. 85, Sep. 1997, pp. 1348-1363.

[3] P. Hough, "Method and means for recognizing complex patterns", U.S. Patent 3,069,654, Dec 1962.

[4] J. Illingworth and J. Kittler, "A survey of the Hough transform", *Computr Vision, Graph. Image Processing*, vol. 44, 1988, pp. 87-116.

[5] J. Cui, Y.Wang, T. Tan, L. Ma, and Z. Sun, "A fast and robust iris localization method based on texture segmentation", *In Proc. SPIE on Biometric Technology for Human Identification*, vol. 5404, 2004, pp. 401-408.

[6] J. Kim, S. Cho, and J. Choi, "Iris recognition using wavelet features", *Journal of VLSI Signal Processing*, vol. 38, 2006, pp. 147-156.

[7] L. Ma, T. Tan, Y.Wang, and D. Zhang, "Efficient Iris Recognition by Characterizing Key Local Variations", *IEEE Trans. on Image Processing*, vol.13, no. 6, 2004, pp.739-750.

[8] J. M. H. Ali and A. E. Hassanien, "An Iris Recognition System to Enhance E-security Environment Based on Wavelet Theory", *Advanced Modeling and Optimization journal*, vol. 5, no. 2, 2003, pp. 93-104.

[9] J. Cui, L. Ma, Y. Wang, T. Tan, Z. Sun, "An Appearance Based Method for IRIS Detection", *Asian Conference on Computer Vision,* vol.2, 2004, pp.1091-1096.

[10] L.R. Kennell, R.W. Ives, R.M. Gaunt, "Binary Morphology and Local Statistics Applied to IRIS Segmentation for Recognition", *IEEE International Conference on Image Processing (ICIP),* 2006.

[11] E.M. Arvacheh, H.R. Tizhoosh, "IRIS Segmentation: Detecting Pupil, Limbus and Eyelids", *IEEE International Conference on Image Processing (ICIP)*, 2006.

[12] X. Guang-Zhu, Z. Zai-Feng, MA Yi-De, "A Novel and Efficient Method for Iris Automatic Location", *Journal of China University of Mining and Technology,* vol. 17, no. 3, 2007, pp.441-446.

[13] CASIA iris image database, http://www.sinobiometrics .com.

[14] S. Dey, D. Samanta, "An Efficient Approach for Pupil Detection in Iris Images", International Conference on Advanced Computing and Communications, Dec. 2007, pp. 382-389.

[15] R.I. Hartley, A. Zisserman, *Multiple View Geometry in Computer Vision*, Second Ed., Cambridge University Press, 2003.

[16] D. H. Ballard and C. M. Brown, *Computer Vision*, Englewood Cliffs, Prentice-Hall, NJ, 1982.

[17] W. K. Pratt, *Digital Image Processing*, Wiley, New York, 1978.

[18] Hugo Proenc¸a and Lu´ıs A. Alexandre, "Ubiris iris image database", http://iris.di.ubi.pt/ubiris2.zip, 2004